
⁸⁹Zr-Bevacizumab PET: Potential Early Indicator of Everolimus Efficacy in Patients with Metastatic Renal Cell Carcinoma

Suzanne C. van Es¹, Adrienne H. Brouwers², Shekar V.K. Mahesh³, Annemarie M. Leliveld-Kors⁴, Igle J. de Jong⁴, Marjolijn N. Lub-de Hooge⁵, Elizabeth G.E. de Vries¹, Jourik A. Gietema¹, and Sjoukje F. Oosting¹

¹Department of Medical Oncology, University Medical Center Groningen, University of Groningen, Groningen, The Netherlands;

²Department of Nuclear Medicine and Molecular Imaging, University Medical Center Groningen, University of Groningen, Groningen, The Netherlands; ³Department of Radiology, University Medical Center Groningen, University of Groningen, Groningen, The Netherlands; ⁴Department of Urology, University Medical Center Groningen, University of Groningen, Groningen, The Netherlands; and ⁵Department of Clinical Pharmacy and Pharmacology, University Medical Center Groningen, University of Groningen, Groningen, The Netherlands

¹Department of Medical Oncology, University Medical Center Groningen, University of Groningen, Groningen, The Netherlands;

Currently, biomarkers that predict the efficacy of everolimus in metastatic renal cell carcinoma (mRCC) patients are lacking. Everolimus inhibits vascular endothelial growth factor A (VEGF-A) expression. We performed PET scans on mRCC patients with ⁸⁹Zr-bevacizumab, a VEGF-A-binding antibody tracer. The aims were to determine a change in tumor tracer uptake after the start of everolimus and to explore whether ⁸⁹Zr-bevacizumab PET can identify patients with early disease progression. **Methods:** ⁸⁹Zr-bevacizumab PET was done before and 2 and 6 wk after the start of everolimus, 10 mg/d, in mRCC patients. Routine CT scans were performed at baseline and every 3 mo thereafter. Tumor tracer uptake was quantified using SUV_{max}. The endpoints were a change in tumor tracer uptake and treatment response on CT after 3 mo. **Results:** Thirteen patients participated. The median SUV_{max} of 94 tumor lesions was 7.3 (range, 1.6–59.5). Between patients, median tumor SUV_{max} varied up to 8-fold. After 2 wk, median SUV_{max} was 6.3 (1.7–62.3), corresponding to a mean decrease of 9.1% ($P < 0.0001$). Three patients discontinued everolimus early. At 6 wk, a mean decrease in SUV_{max} of 23.4% compared with baseline was found in 70 evaluable lesions of 10 patients, with a median SUV_{max} of 5.4 (1.1–49.4, $P < 0.0001$). All 10 patients who continued treatment had stable disease at 3 mo. **Conclusion:** Everolimus decreases ⁸⁹Zr-bevacizumab tumor uptake. Further studies are warranted to evaluate the predictive value of ⁸⁹Zr-bevacizumab PET for everolimus antitumor efficacy.

Key Words: molecular imaging; positron emission tomography; renal cell carcinoma; everolimus; biomarker

J Nucl Med 2017; 58:905–910

DOI: 10.2967/jnumed.116.183475

Clear cell renal cell carcinoma (RCC) is characterized by Von Hippel–Lindau gene inactivation. This results in expression of proangiogenic growth factors such as vascular endothelial growth

factor A (VEGF-A) and typical vascular tumors. Patients with RCC have higher circulating VEGF-A levels than healthy controls (1). A high baseline plasma VEGF-A level is associated with shorter progression-free survival (PFS) and overall survival (OS) in metastatic RCC (mRCC) and is an independent prognostic factor (2). VEGF-A pathway-targeting agents such as the VEGF-A-binding antibody bevacizumab with interferon alfa or the tyrosine kinase inhibitors sunitinib, sorafenib, pazopanib, and axitinib are established treatment options for mRCC (3–6). Inhibitors of mammalian target of rapamycin (mTOR) also have antitumor activity in mRCC (7,8). mTOR plays a key role in cell growth, protein translation, autophagy, and metabolism. Blocking mTOR causes cell cycle arrest in a broad range of tumor types, but in addition to a direct antitumor effect, mTOR inhibitors block VEGF-A expression, vascular permeability, endothelial cell proliferation, and angiogenesis (9).

Everolimus is an orally administered mTOR inhibitor. A phase III study in mRCC patients with progressive disease during or after treatment with sunitinib, sorafenib, or both demonstrated doubling of median PFS for everolimus compared with placebo (4.9 mo vs. 1.9 mo) (10). Recently, nivolumab was proven to be superior to everolimus in pretreated mRCC patients, with median OS of 25.0 mo compared with 19.6 mo, and fewer high-grade, treatment-related adverse events (11).

Only a subset of mRCC patients profits from treatment with mTOR inhibitors. Regrettably, no predictive biomarkers that can identify patients who are likely to benefit from mTOR inhibitors are available. The novel treatment option with the immunotherapeutic drug nivolumab after first-line antiangiogenic treatment further reinforces the need for such a predictive biomarker. ⁸⁹Zr-bevacizumab is a PET tracer that binds VEGF-A. We demonstrated in a previous study that ⁸⁹Zr-bevacizumab PET scans can visualize RCC tumor lesions and that tracer uptake in these lesions changed during treatment with sunitinib or bevacizumab/interferon alfa. Furthermore, results suggested that high baseline tumor uptake was associated with a longer time to progression (12). Serial ⁸⁹Zr-bevacizumab PET scans might also be useful to assess downregulation of tumor VEGF-A expression after the start of an mTOR inhibitor and serve as an early indicator of efficacy. We hypothesize that successful downregulation of VEGF-A expression by everolimus results in a decrease in tumor tracer uptake after the start of treatment.

Received Sep. 1, 2016; revision accepted Oct. 24, 2016.

For correspondence or reprints contact: Sjoukje F. Oosting, Department of Medical Oncology, University Medical Center Groningen, University of Groningen, P.O. Box 30 001, 9700 RB Groningen, The Netherlands.

E-mail: s.oosting@umcg.nl

Published online Jan. 12, 2017.

COPYRIGHT © 2017 by the Society of Nuclear Medicine and Molecular Imaging.

We conducted a feasibility study in patients with mRCC who started treatment with everolimus. The primary objective of this study was to demonstrate a change in tumor tracer uptake after the start of treatment. The secondary objective was to explore whether ^{89}Zr -bevacizumab PET could identify patients with disease progression on the first follow-up CT scan after 3 mo of treatment.

MATERIALS AND METHODS

Patients

Adult mRCC patients who had measurable disease, had a World Health Organization performance score of 2 or less, and were candidates to start treatment with everolimus were eligible. The study was approved

by the institutional review board, and all subjects gave written informed consent. The trial is registered on ClinicalTrials.gov (NCT01028638).

Study Design and Treatment

Patients underwent ^{89}Zr -bevacizumab PET imaging before and 2 and 6 wk after the start of everolimus, 10 mg orally once daily. Treatment was continued until disease progression or unacceptable toxicity. The primary endpoint was a change in ^{89}Zr -bevacizumab uptake in tumor lesions between the baseline PET scan and the scans after 2 and 6 wk of treatment. The secondary endpoint was progressive disease according to RECIST 1.1 after 3 mo of treatment.

Imaging Techniques

Four days before each PET scan, the patients were injected intravenously with 37 MBq of ^{89}Zr -bevacizumab, protein dose 5 mg. No therapeutic effects are to be expected from this dose because therapeutic bevacizumab doses vary from 7.5 to 15 mg per kilogram of body weight. Conjugation and labeling were done as described before (13). The patients were scanned from head to upper thigh in up to 8 consecutive bed positions as described earlier (12), with a final reconstruction resolution of about 10 mm.

At baseline and every 3 mo during treatment, the patients underwent CT imaging. CT was performed with oral and intravenous contrast and a maximal slice thickness of 5.0 mm. The mean interval between the baseline CT and baseline PET scans was 15 d.

Imaging Data Analysis

The baseline PET scans were fused with the baseline CT scans and analyzed by visual and quantitative assessment of tumor lesions. All hot spots on PET that were concordant with tumor lesions on CT were documented as being metastases. For reliable quantification of ^{89}Zr -bevacizumab uptake, lesions had to be larger than 10 voxels and had to be delineable from normal-organ background. Irradiated lesions were excluded from quantification. Quantification was performed with AMIDE Medical Image Data Examiner software (version 0.9.1; Stanford University) (14). SUV_{max} and SUV_{mean} were calculated for tumor lesions and healthy organs. SUV_{max} and SUV_{mean} correlated strongly ($r = 0.99$, $P < 0.0001$) (Supplemental Fig. 1; supplemental materials are available at <http://jnm.snmjournals.org>). SUV_{max} is less operator-dependent and was therefore used for calculations of tumor tracer uptake. SUV_{mean} was used for measuring uptake in healthy organs. CT findings were evaluated by a radiologist. All tumor lesions measuring at least 10 mm on the baseline CT scan were noted for comparison with PET. Treatment response was assessed according to RECIST 1.1.

TABLE 1

Patient Demographics and Clinical Characteristics

Variable	Data
Sex	
Male	9 (69.2)
Female	4 (30.8)
Age (y)	63 (51–71)
Nephrectomy	
Yes	11 (84.6)
No	2 (15.4)
Histology	
Pure clear cell	12 (92.3)
Mixed	1 (7.7)
World Health Organization performance	
0	4 (30.8)
1	2 (15.4)
2	7 (53.8)
Tumor sites	
Number	4 (2–7)
Kidney	6 (46.2)
Primary	2 (15.4)
Local recurrence	2 (15.4)
Contralateral	2 (15.4)
Lung	9 (69.2)
Lymph node	7 (53.8)
Bone	6 (46.2)
Liver	5 (38.5)
Adrenal	4 (30.8)
Muscle	4 (30.8)
Other	10 (76.9)
Previous treatment	
Tyrosine kinase inhibitor	8 (61.5)
Tyrosine kinase inhibitor and interferon alfa ± bevacizumab	2 (15.4)
Other	3 (23.1)

Qualitative data are expressed as number followed by percentage in parentheses; continuous data are expressed as median followed by range in parentheses.

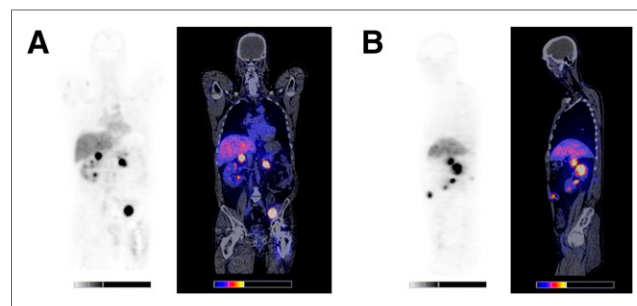


FIGURE 1. Baseline ^{89}Zr -bevacizumab PET images of mRCC patient. (A) Coronal 2-dimensional image through right adrenal gland metastasis, showing additionally 1 local recurrence in left kidney tumor, 1 kidney metastasis, and 1 soft-tissue metastasis near left iliac bone. (B) Sagittal 2-dimensional image through right adrenal gland metastasis, showing additionally 3 kidney metastases and 1 soft-tissue metastasis in abdominal wall.

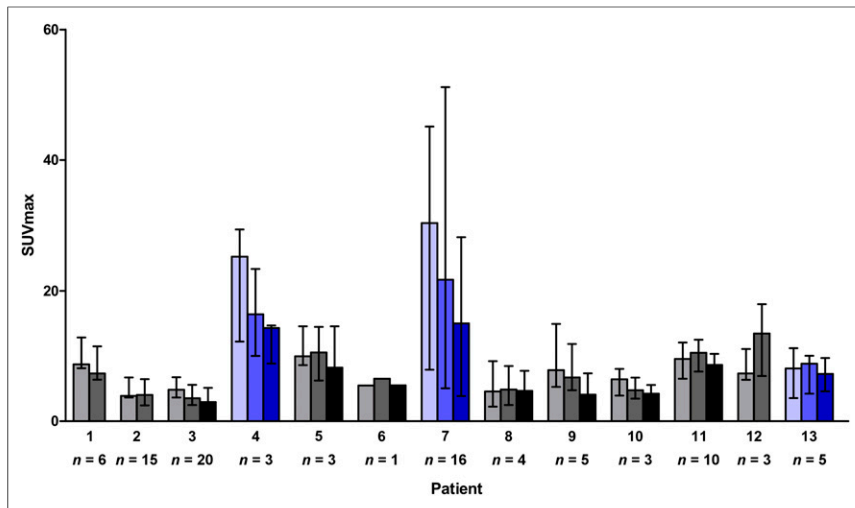


FIGURE 2. Median tumor tracer uptake with interquartile range per patient at baseline (light shading), after 2 wk of everolimus (medium shading), and after 6 wk of treatment (dark shading). Patients in blue stayed on treatment > 12 mo. n = number of quantified tumor lesions per patient.

Biomarker Analysis

Serum samples were collected before every tracer injection—for analysis of circulating VEGF-A levels, with day 0 being the day of the baseline PET scan and the start of everolimus treatment. The blood was centrifuged, and platelet-poor plasma samples were stored at -80°C until analysis. VEGF-A was analyzed using an enzyme-linked immunosorbent assay (R&D Systems). Plasma VEGF-A was compared with tumor tracer uptake.

Statistical Assessments

We estimated that to predict with 80% power (2-sided $\alpha = 0.05$) that there is a true difference in SUV (≥ 1.25 SD) between the baseline

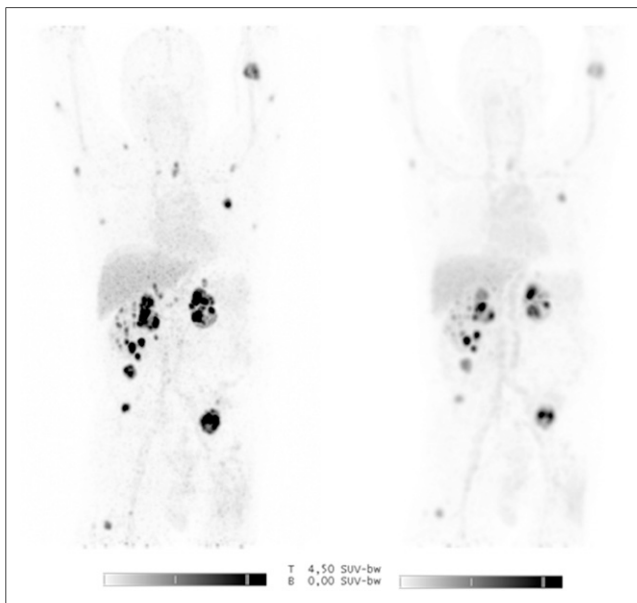


FIGURE 3. (Left) Maximum-intensity projection before treatment showing multiple local recurrences in left kidney tumor and metastases in right kidney, right adrenal gland, and soft-tissue. (Right) Maximum-intensity projection after 6 wk of treatment showing heterogeneous decrease in uptake.

scan and the scan after 2 or 6 wk, the required number of patients would be 11. The change in ^{89}Zr -bevacizumab tumor lesion uptake between the baseline scan and the scan after 2 or 6 wk of treatment was calculated and presented as a percentage (mean with 95% confidence interval). The Wilcoxon paired rank test was used to assess the significance of the change in tumor and healthy organ tracer uptake and plasma VEGF-A. Correlations were analyzed using the Spearman rank test.

Analyses were performed with SPSS, version 22 (IBM).

RESULTS

Patients

Between December 2009 and October 2014, 13 patients were included. The median interval between the stopping of tyrosine kinase inhibitor and the starting of everolimus was 10.57 wk, with a mean of 16.8 wk (range, 2–44.3 wk). Ten patients

completed the study; 2 patients stopped everolimus between 2 and 6 wk because of adverse events, and one patient had clinically progressive disease before the third PET scan. The median time to progression was 5.8 mo (range, 1.9–24.9 mo). The patient characteristics are presented in Table 1.

^{89}Zr -Bevacizumab PET

^{89}Zr -Bevacizumab Uptake in Tumor Lesions. ^{89}Zr -bevacizumab PET images were of high quality and visualized tumor lesions clearly (Fig. 1). Of 147 tumor lesions 10 mm or larger on CT, 103 were detected as hot spots on the PET scan (71%). A total of 94 tumor lesions fulfilled the criteria for reliable quantification and were used for calculations (Fig. 2).

The median SUV_{max} at baseline was 7.3 (range, 1.6–59.5). All 13 patients underwent the second PET scan after 2 wk of treatment. The median SUV_{max} was 6.3 (range, 1.7–62.3), corresponding to a mean change of -9.1% (95% confidence interval, -3.4% to -14.9% , $P < 0.0001$). On the third PET scan, performed on 10 patients, 70 evaluable lesions were apparent, with a median SUV_{max} of 5.4 (range, 1.1–49.4). This corresponds to a mean change of -23.4% (95% confidence interval, -16.5% to -30.2% , $P < 0.0001$) compared with baseline (Figs. 3–5).

^{89}Zr -Bevacizumab Uptake in Healthy Organs. ^{89}Zr -bevacizumab uptake in healthy organs at baseline was comparable to previous studies (Supplemental Fig. 2) (12,15).

^{89}Zr -Bevacizumab PET and Treatment Outcome. All 10 patients still on everolimus after 3 mo had stable disease according to RECIST 1.1 at the first response evaluation. The single patient with clinical progressive disease within 3 mo had a baseline median tumor SUV_{max} of 8.7 (range, 6.8–14.9) and a mean decrease of 12.2% in tumor SUV_{max} after 2 wk of treatment, which resembles the pattern seen in patients without early progression. Exploratory analysis showed a correlation between baseline mean tumor SUV_{max} and time on treatment ($r = 0.63$, $P = 0.02$, Supplemental Fig. 3). The mean tumor SUV_{max} at baseline of patients who were on treatment longer than 12 mo was higher than the mean tumor SUV_{max} of patients who were on treatment less than 12 mo (median mean tumor SUV_{max} , 22.2 vs. 7.2) ($P = 0.09$).

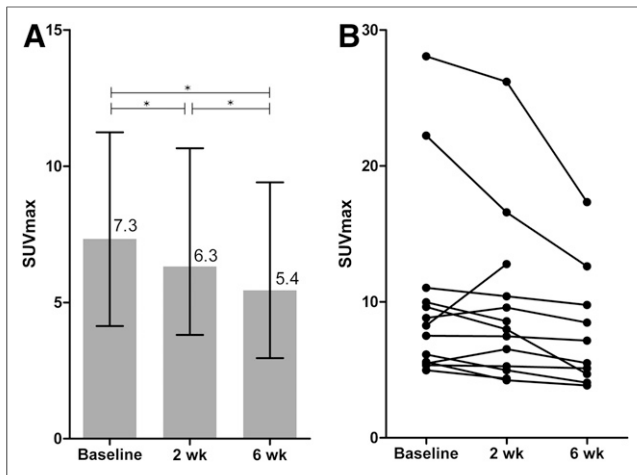


FIGURE 4. Tumor tracer uptake before and during treatment. (A) Median uptake and interquartile range for all lesions. (B) Mean tumor uptake per patient. * $P < 0.0001$.

There was no correlation between change in SUV_{max} after 2 and 6 wk of treatment and time on treatment.

Plasma VEGF-A. The median baseline plasma VEGF-A was 408 pg/mL ($n = 13$; range, 144–2,013 pg/mL). At day 11, the median plasma VEGF-A was 97 pg/mL ($n = 12$; range, <38–644 pg/mL), representing a mean decrease of 68.7% ($P = 0.001$). After 6 wk, 10 patients were ongoing, and 9 samples were available. The median VEGF-A was 83 pg/mL (range, <38–384 pg/mL; decrease, 74.6%; $P = 0.004$) (Fig. 6). Only one patient showed an increase in plasma VEGF-A level after 2 wk of treatment; this patient had early clinical progression. At baseline, there was no correlation

between plasma VEGF-A and tumor SUV_{max} . There was also no correlation between change in tumor tracer uptake and change in plasma VEGF-A after 2 or 6 wk.

DISCUSSION

In this study on mRCC patients, we found a decrease in ^{89}Zr -bevacizumab tumor uptake after 2 wk of everolimus treatment and a further decrease after 6 wk. Because all patients had stable disease on CT at 3 mo, we could not assess the use of ^{89}Zr -bevacizumab PET for early identification of progressive disease. Substantial heterogeneity in tumor tracer uptake both within and between patients was seen at baseline, but also the change in tumor tracer uptake during treatment varied considerably.

Predictive biomarkers that can differentiate between patients likely to benefit from mTOR inhibitors and those unlikely to benefit are needed to achieve patient-tailored therapy. Several potential markers have been identified, such as functional mutations in the mTOR pathway genes, baseline serum lactate dehydrogenase, and off-target effects resulting in specific side effects (16–19). However, these markers still have to be validated, and their potential clinical usefulness has to be established.

^{18}F -FDG PET has been investigated as a predictive biomarker for everolimus treatment in 50 mRCC patients. There was no correlation between baseline SUV_{max} and change in tumor size, but baseline SUV_{max} showed a significant negative correlation with OS and PFS. A modest correlation between change in SUV_{max} and change in tumor size was found, but change in SUV_{max} did not correlate with OS or PFS. Altogether, the investigators did not recommend any additional studies (20).

We developed ^{89}Zr -bevacizumab PET imaging to noninvasively study tumor VEGF-A concentration. Previously, we performed

serial ^{89}Zr -bevacizumab PET scans (at baseline and after 2 and 12 wk) on patients who started everolimus treatment for neuroendocrine tumors (15). In that study, tumor lesions were visualized in 10 of 14 patients, with a median SUV_{max} of 5.8 (range, 1.7–15.1). Tumor SUV_{max} decreased by 7% after 2 wk of treatment and by 35% after 12 wk, which mirrors the results of the current study on mRCC patients. The highest tumor SUV_{max} in neuroendocrine tumor patients, however, was 15.1, whereas in the current study on mRCC patients the highest was 59.5. Furthermore, only 19% of all lesions 10 mm or larger were visualized in the 10 neuroendocrine tumor patients with a positive PET scan, whereas in the present study we visualized 71% of mRCC lesions 10 mm or larger. These differences are likely explained by tumor biology. Sporadic VHL mutations are a unique characteristic of RCC and result in high VEGF-A production by tumor cells.

In the current study we did not perform biopsies. However, a good correlation between tumor uptake of radioactive labeled bevacizumab and VEGF-A in tumor tissue was shown earlier (13,21,22). We therefore

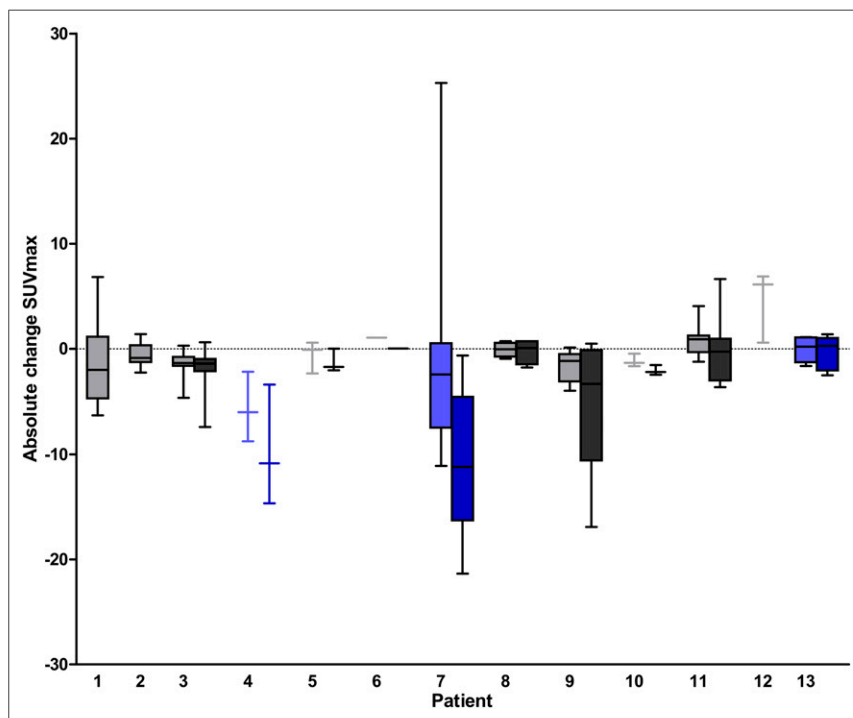


FIGURE 5. Absolute SUV_{max} change with median for all lesions per patient after 2 wk (light shading) and 6 wk (dark shading) of everolimus treatment. Patients in blue stayed on treatment > 12 mo.

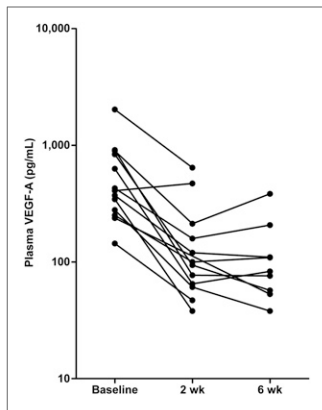


FIGURE 6. Plasma VEGF-A concentrations. Each line represents one patient.

of everolimus are visualized with serial ^{89}Zr -bevacizumab PET remains to be determined.

Patients who participated in the current study received prior treatment with a tyrosine kinase inhibitor. In a previous study, we demonstrated that sunitinib results in a heterogeneous change in tumor ^{89}Zr -bevacizumab uptake, with an overall slight decrease and a rebound phenomenon after 2 stop weeks (12). The median interval between the stopping of tyrosine kinase inhibitor and the starting of everolimus was 10.57 wk (range, 2–44.3 wk). For the 2 patients who had an interval of 2 wk between tyrosine kinase inhibitor and tracer injection, we cannot exclude the possibility that prior treatment influenced tumor tracer uptake. For the overall study results, however, any influence from previous treatment is likely limited.

Median plasma VEGF-A decreased after 2 wk of everolimus treatment. Overall, a small further decrease was measured after 6 wk, but in half the patients plasma VEGF-A increased between weeks 2 and 6.

The current study was conducted before publication of the CheckMate 025 and METEOR trials (11,25). Nivolumab, a programmed-death-1-targeting antibody that acts as an immune checkpoint inhibitor, prolonged OS compared with everolimus in previously treated patients with advanced RCC. Cabozantinib, a tyrosine kinase inhibitor of VEGF receptors, MET, and AXL, was also shown to be superior to everolimus in previously treated mRCC patients. These trials strongly enforce the need for predictive biomarkers that can identify patients who will likely benefit from everolimus to allow individualized treatment choices. In an exploratory analysis, we found that the baseline ^{89}Zr -bevacizumab PET results correlated with time on treatment. Tumor tracer uptake was higher in patients who were treated longer. Therefore, ^{89}Zr -bevacizumab PET might be useful for predicting treatment success.

Previously, we published results on serial ^{89}Zr -bevacizumab PET imaging of mRCC patients who were treated with bevacizumab/interferon alfa or sunitinib. A similar heterogeneous tumor tracer uptake at baseline was found with a slightly lower detection rate of tumor lesions 10 mm or larger (56.7%). A correlation between baseline tumor tracer uptake and time to progression was shown in an exploratory analysis, with a high uptake corresponding to a longer time to progression (12). This observation, in combination with the current study, supports the option that ^{89}Zr -bevacizumab

assume that the decrease in tumor tracer uptake represents a reduction in VEGF-A production by the tumor cells as a result of everolimus treatment. Another potential explanation may be antiangiogenic effects of everolimus, such as reduced tumor perfusion or reduced vascular permeability (23). However, dynamic contrast-enhanced MRI using K^{trans} measurement in patients with advanced cancer showed no decrease in tumor perfusion on everolimus treatment (24). Whether mainly tumor VEGF-A concentration or also antiangiogenic effects

PET has prognostic rather than predictive value. Interestingly, in nephrectomy samples from 137 patients with locally advanced or metastatic clear cell RCC, high VEGF expression determined by immunohistochemistry was associated with worse OS. Median OS was 206 mo in patients with low VEGF expression and 65 mo in patients with high VEGF expression ($P < 0.001$) (26). This observation raises the possibility that high tumor VEGF-A is an unfavorable prognostic factor but—in the metastatic setting, by providing a target for treatment—identifies patients that show prolonged benefit from direct and indirect VEGF pathway inhibition with angiogenesis and mTOR inhibitors.

Larger trials are needed to evaluate whether this molecular imaging tool can serve as a predictive biomarker to select patients who derive clinically relevant benefit from everolimus.

CONCLUSION

^{89}Zr -bevacizumab tumor uptake decreases significantly during everolimus treatment in mRCC patients. We could not demonstrate whether ^{89}Zr -bevacizumab PET can be used for early identification of progressive disease. Larger trials are warranted to determine whether ^{89}Zr -bevacizumab PET can be used to select patients for everolimus treatment.

DISCLOSURE

This work was supported by Novartis and the Dutch Cancer Society (RUG 2012-5565). No other potential conflict of interest relevant to this article was reported.

REFERENCES

- Schips L, Dalpiaz O, Lipsky K, et al. Serum levels of vascular endothelial growth factor (VEGF) and endostatin in renal cell carcinoma patients compared to a control group. *Eur Urol*. 2007;51:168–173.
- Escudier B, Eisen T, Stadler WM, et al. Sunitinib for treatment of renal cell carcinoma: final efficacy and safety results of the phase III Treatment Approaches in Renal Cancer Global Evaluation Trial. *J Clin Oncol*. 2009;27:3312–3318.
- Escudier B, Pluzanska A, Koralewski P, et al. Bevacizumab plus interferon alfa-2a for treatment of metastatic renal cell carcinoma: a randomised, double-blind phase III trial. *Lancet*. 2007;370:2103–2111.
- Motzer RJ, Hutson TE, Tomczak P, et al. Sunitinib versus interferon alfa in metastatic renal-cell carcinoma. *N Engl J Med*. 2007;356:115–124.
- Motzer RJ, Hutson TE, Cella D, et al. Pazopanib versus sunitinib in metastatic renal-cell carcinoma. *N Engl J Med*. 2013;369:722–731.
- Rini BI, Escudier B, Tomczak P, et al. Comparative effectiveness of axitinib versus sorafenib in advanced renal cell carcinoma (AXIS): a randomised phase 3 trial. *Lancet*. 2011;378:1931–1939.
- Hudes G, Carducci M, Tomczak P, et al. Temsirolimus, interferon alfa, or both for advanced renal-cell carcinoma. *N Engl J Med*. 2007;356:2271–2281.
- Motzer RJ, Escudier B, Oudard S, et al. Efficacy of everolimus in advanced renal cell carcinoma: a double-blind, randomised, placebo-controlled phase III trial. *Lancet*. 2008;372:449–456.
- Meric-Bernstam F, Gonzalez-Angulo AM. Targeting the mTOR signaling network for cancer therapy. *J Clin Oncol*. 2009;27:2278–2287.
- Motzer RJ, Escudier B, Oudard S, et al. Phase 3 trial of everolimus for metastatic renal cell carcinoma: final results and analysis of prognostic factors. *Cancer*. 2010;116:4256–4265.
- Motzer RJ, Escudier B, McDermott DF, et al. Nivolumab versus everolimus in advanced renal-cell carcinoma. *N Engl J Med*. 2015;373:1803–1813.
- Oosting SF, Brouwers AH, van Es SC, et al. ^{89}Zr -bevacizumab PET visualizes heterogeneous tracer accumulation in tumor lesions of renal cancer patients and differential effects of anti-angiogenic treatment. *J Nucl Med*. 2015;56:63–69.
- Gaykema SB, Brouwers AH, Lub-de Hooge MN, et al. ^{89}Zr -bevacizumab PET imaging in primary breast cancer. *J Nucl Med*. 2013;54:1014–1018.

14. Loening AM, Gambhir SS. AMIDE: a free software tool for multimodality medical image analysis. *Mol Imaging*. 2003;2:131–137.
15. van Asselt SJ, Oosting SF, Brouwers AH, et al. Everolimus reduces ⁸⁹Zr-bevacizumab tumor uptake in patients with neuroendocrine tumors. *J Nucl Med*. 2014;55:1087–1092.
16. Voss MH, Hakimi AA, Pham CG, et al. Tumor genetic analyses of patients with metastatic renal cell carcinoma and extended benefit from mTOR inhibitor therapy. *Clin Cancer Res*. 2014;20:1955–1964.
17. Armstrong AJ, Georje DJ, Halabi S. Serum lactate dehydrogenase predicts for overall survival benefit in patients with metastatic renal cell carcinoma treated with inhibition of mammalian target or rapamycin. *J Clin Oncol*. 2012;30:3402–3407.
18. Dabydeen DA, Jagannathan JP, Ramaiya N, et al. Pneumonitis associated with mTOR inhibitors therapy in patients with metastatic renal cell carcinoma: incidence, radiographic findings and correlation with clinical outcome. *Eur J Cancer*. 2012;48:1519–1524.
19. Lee CK, Marschner IC, Simes RJ, et al. Increase in cholesterol predicts survival advantage in renal cell carcinoma patients treated with temsirolimus. *Clin Cancer Res*. 2012;18:3188–3196.
20. Chen JL, Appelbaum DE, Kocherginsky M, et al. FDG-PET as a predictive biomarker for therapy with everolimus in metastatic renal cell cancer. *Cancer Med*. 2013;2:545–552.
21. van der Bilt AR, Terwisscha van Scheltinga AG, Timmer-Bosscha H, et al. Measurement of tumor VEGF-A levels with ⁸⁹Zr-bevacizumab PET as an early biomarker for the antiangiogenic effect of everolimus treatment in an ovarian cancer xenograft model. *Clin Cancer Res*. 2012;18:6306–6314.
22. Nagengast WB, Hooge MN, van Straten EM, et al. VEGF-SPECT with ¹¹¹In-bevacizumab in stage III/IV melanoma patients. *Eur J Cancer*. 2011;47:1595–1602.
23. Phung TL, Ziv K, Dabydeen D, et al. Pathological angiogenesis is induced by sustained Akt signaling and inhibited by rapamycin. *Cancer Cell*. 2006;10:159–170.
24. Ciunci CA, Perini RF, Avadhani AN, et al. Phase I and pharmacodynamic trial of everolimus in combination with cetuximab in patients with advanced cancer. *Cancer*. 2014;120:77–85.
25. Choueiri TK, Escudier B, Powles T, et al. Cabozantinib versus everolimus in advanced renal-cell carcinoma. *N Engl J Med*. 2015;373:1814–1823.
26. Minardi D, Santoni M, Lucarini G, et al. Tumor VEGF expression correlates with tumor stage and identifies prognostically different group in patients with clear cell renal cell carcinoma. *Urol Oncol*. 2015;33:113.e1–113.e7.